Divergent Roles of Nucleus Accumbens D1- and D2-MSNs in Regulating Hedonic Feeding

Running title: NAc MSNs and Hedonic Feeding

Chase A. Carter[1]*, Gaby M. Soden[2]*, Samhitha S. Pudipeddi[1], Pierre Llorach[2], Jessica J. Walsh[2], Daniel J. Christoffel[1]

[1]Department of Psychology and Neuroscience, [2]Department of Pharmacology,
The University of North Carolina at Chapel Hill, North Carolina 27599
*These authors contributed equally to this work
Corresponding author: Daniel Christoffel
Email: dchristoffel@unc.edu

Number of pages: 19
Number of figures: 5
Number of words for abstract (200), introduction (648), and discussion (1248)
Conflict of interest statement: "The authors declare no competing financial interests."
Acknowledgments: This work was supported by NIH Grants T32GM12274 (G.M.S.) and R00 DK115985 (D.J.C.) and a BBRF Young Investigator Award (D.J.C). We thank all members of the Christoffel and Walsh lab for their support and helpful discussion surrounding this project.

Abstract

The nucleus accumbens (NAc) is a critical node in the neural circuitry underlying reward and motivated behavior, including hedonic feeding, and its dysfunction is implicated in maladaptive behaviors in numerous psychiatric disorders. Medium spiny neurons (MSNs) in the NAc are predominantly categorized into dopamine 1 receptor-expressing (D1-MSNs) and dopamine 2 receptor-expressing (D2-MSNs) subtypes, which are thought to exert distinct and sometimes opposing roles in reward-related processes. Here, we used optogenetic, chemogenetic, and fiber photometry approaches in Cre-driver mouse lines to dissect the causal contributions of D1- and D2-MSNs to the consumption of a high-fat diet in sated animals. Activation of D1-MSNs via optogenetics or DREADDs significantly suppressed high-fat intake, whereas inhibition of these neurons increased consumption. Conversely, activation of D2-MSNs enhanced high-fat food intake, while their inhibition reduced intake. Fiber photometry revealed dynamic shifts in D2-MSN activity over repeated high-fat exposures, with increasing activity correlating with escalating intake. These results highlight opposing contributions of D1- and D2-MSN populations in regulating hedonic feeding and support a model in which motivational salience and consumption are modulated by MSN subtype-specific activity in the NAc. Understanding this circuitry has implications for the development of targeted treatments for obesity and other disorders of compulsive consumption.

Significance Statement

Obesity and metabolic disorders are partly driven by dysregulated motivation for palatable foods, yet the neural circuits underlying hedonic feeding are not fully understood. This study shows that nucleus accumbens (NAc) medium spiny neurons (MSNs) have opposing roles in high-fat food intake during early exposure: D1-MSNs suppress, while D2-MSNs promote, consumption in sated mice. Using chemogenetics, optogenetics, and fiber photometry, we establish a causal link between MSN activity and hedonic feeding. These findings challenge simplified models of reward processing and highlight the experience-dependent roles of MSN subtypes. By defining cell-type-specific contributions to non-homeostatic eating, this work offers key insight into the neural basis of compulsive intake and informs strategies for targeted intervention in obesity and related conditions.

Introduction

Neurons implicated in homeostatic feeding directly and indirectly interface with circuits that influence reward and aversion (Marinescu and Labouesse, 2024). The nucleus accumbens (NAc), a key component of the mesolimbic reward circuitry, critically mediates motivated behaviors, including hedonic feeding or the consumption of palatable foods in the absence of metabolic need, which significantly contributes to the rising rates of obesity (Volkow and Wise, 2005; Kenny, 2011; Sharma et al., 2012; Brown et al., 2015; Ferrario, 2017; DiFeliceantonio and Small, 2019). This region serves as a critical integration hub, receiving a diverse array of excitatory, inhibitory, and neuromodulatory inputs that converge onto its principal output neurons, the medium spiny neurons (MSNs) (Mogenson et al., 1980; Castro and Bruchas, 2019).

The prominent regulatory role of NAc activity in feeding was established by early investigations which demonstrated increased food intake in sated rodents following pharmacological inhibition of the NAc. A majority of NAc neuron are inhibited during consumption, suggesting theses "pauses" encode the motor act of initiating consumption (Kelley, 2004; Taha and Fields, 2005, 2006). Interestingly, a distinct subset of NAc neurons exhibit increased firing during intake and appear to encode the palatability and value of food rewards (Roitman et al., 2005; Taha and Fields, 2005, 2006; Krause et al., 2010). Later studies found that acute high-fat diet consumption activates cFos expression in the NAc, indicating its involvement in the mesolimbic response to rewarding food stimuli (Valdivia et al., 2014). Further, NAc MSNs also undergo diet-induced plasticity and display increased excitability in obesity prone rats chronically exposed to a calorically-dense, palatable diet (Ferrario, 2017; Oginsky and Ferrario, 2019; Ferrario et al., 2024).

MSNs are canonically classified into two main subtypes based on their dopamine receptor expression: dopamine 1 receptor-expressing (D1-MSNs) and dopamine 2 receptor-expressing (D2-MSNs). These distinct neuronal populations have been implicated in dissociable roles in motivated behavior, with D1-MSNs often associated with the promotion of action and reward seeking, while D2-MSNs are frequently linked to inhibitory control and aversion (Russo and Nestler, 2013; Steinberg et al., 2015). However, the functional contributions of these MSN subtypes are increasingly recognized as more nuanced and not strictly dichotomous. It appears that the specific contributions of MSN subtypes in regulating feeding behavior seem to depend on diet valence and context, as well as NAc subregion (core vs shell). Recent studies offer conflicting findings regarding the role of D1-MSNs in feeding behavior. While some report that acute inhibition of D1-MSNs increases food intake, others demonstrate that enhanced D1-MSN activity promotes food consumption, food-seeking behavior, and contributes to diet-induced weight gain (O'Connor et al., 2015; Zhu et al., 2016; Matikainen-Ankney et al., 2023; Walle et al., 2024). The function of D2-MSNs remains less clearly defined. Some studies report no significant effect of manipulating their activity, whereas others show that D2-MSN activity increases during feeding, exhibits context-

dependent effects, and is altered by chronic exposure to palatable diets, including changes in D2R expression (Johnson and Kenny, 2010; Zhu et al., 2016; Walle et al., 2024).

In this study, we used a combination of chemogenetic and optogenetic tools in transgenic mouse lines to selectively modulate D1- and D2-MSN activity during limited access to high-fat food in sated animals. In line with previous findings (Marinescu and Labouesse, 2024), we find that repeated activation of D1-MSNs during multiple days of high-fat exposure suppressed intake, while their inhibition increased consumption. In contrast, activation of D2-MSNs enhanced high-fat intake, and inhibition suppressed it. Complementary fiber photometry experiments revealed an experience-dependent increase in D2-MSN activity during high-fat consumption over repeated exposures. These findings demonstrate that D1- and D2-MSNs exert opposing influences on hedonic feeding, with D1-MSNs acting to suppress and D2-MSNs promote palatable food intake. By identifying distinct regulatory roles for MSN subtypes in feeding, this work provides critical insight into the functional organization of the NAc and highlights potential cellular targets for intervention in obesity and compulsive overeating.

Materials and Methods

Animals: All transgenic mice (Drd1a-Cre (FK150, GENSAT; Gong et al., 2007), Adora2a-Cre (KG139, GENSAT) were bred in-house on a C57Bl/6J background. Hemizygous male and female mice were used for all experiments. Mice of the same sex were group-housed on a 12-h light/dark schedule (lights on at 7am) in a vivarium maintained at 22° C with food and water ad libitum unless otherwise noted. House chow contained 26% protein, 60% carbohydrates, and 14% fat by calories (4.17 kcal/g: Prolab® RMH 3000, Purina LabDiet®; St. Louis, MO). The high fat-diet used to model binge-eating contained 20% protein, 20% carbohydrates, and 60% fat by calories (5.24 kcal/g: Research Diets). No statistical methods were used to predetermine sample size. All procedures were approved by the University of North Carolina Institutional Animal Care and Use Committee and followed the Guidelines for the Care and Use of Laboratory Animals.

Blinding: All experiments were conducted in a blinded manner such that assays were conducted and analyzed without knowledge of the specific manipulation being performed and with animals being randomized by cage before surgery and behavioral experiments. Animals were excluded from analysis for behavioral results following postmortem histological verification of viral expression and placement.

Surgery: Mice were anesthetized with a ketamine (100 mg/kg)-xylazine(1 mg/kg) mixture, mounted in a stereotaxic frame and the skull surface was exposed. Thirty-three gauge syringe needles (Hamilton) were used to infuse 0.3 µl of virus into the NAc (angle 10°, anteroposterior 1.6, mediolateral ± 1.5, dorsoventral −4.4) at a rate of 0.1 µl/min. Needles were removed 5 min after infusions were complete. For fiber photometry, fiberoptic implants (400 µm core, NA – 0.66; Doric) and for optogenetics in-house made ferrules (200 µm core, NA – 0.44)

were implanted above the NAc (angle 10°, anteroposterior 1.6, mediolateral ± 1.5, dorsoventral −4.3) unilaterally for photometry and bilaterally for optogenetics. To secure ferrules, miniature screws (thread size 00–90 × 1/16, Antrin Miniature Specialties) were inserted into the skull, and light-cured dental adhesive cement (Geristore A&B paste, DenMat) was applied over the skull surface and base of ferrules.

Viruses: Adeno-associated viruses (AAV) used in this study purchased from Addgene and UNC Vector Core included: Addgene - pAAV8-hSyn-DIO-EGFP, #50457-AAV8; pAAV8-hSyn-DIO-HA-hM3D(Gi)-IRE8-mCitrine, #50455-AAV8; pAAV8-hSyn-DIO-HA-hM3D(Gq)-IRE8-mCitrine, # 50454-AAV8; UNC Vector Core – rAAV2/ EF1a-DIO-EYFP, # AV4842F; rAAV2/ EF1a-DIO-hChR2(H134R)-EYFP, #AV4378P; rAAV5/P AAV-Ef1a-DIO-GCaMP6m, #AV7599. AAV titers ranged from 4.4×10^{12} to 2.4×10^{13} gc/ml.

High-fat intake: Mice were group housed during the period of exposure to high-fat chow. High-fat chow was administered in a similar manner as previously described (Wu et al., 2018; Christoffel et al., 2021a) . In brief, weight-matched mice were randomly assigned to each experimental condition. Group housed mice were separated and acclimated to the familiar cage for 30 min prior to each high-fat exposure. A single, pre-weighed high-fat pellet was provided to the mice in their familiar cage at the same time each day for a given experiment. Intake of the high-fat diet within that period was measured by subtracting the post-exposure weight from the pre-exposure weight. This amount was then converted to calories (1g of high-fat contains 5240 calories) and then divided by the animal's body weight (BW) to generate the calories per gram of BW consumed (cal/g). For all chemogenetic and optogenetic experiments, mice were fed high-fat daily for a 20 min period for 4 consecutive days. For fiber photometry behavioral experiments, high-fat was administered for 1 hour daily with photometric recordings occurring on days 1 and 4. All mice with appropriate expression and targeting were included in data presentation and analyses.

Optogenetic stimulation: D1-Cre+ mice expressing either ChR2 or a control eYFP virus received blue light stimulation (~460 nm, Prizmatix) via optic ferrules implanted above the NAc. Light was delivered through a bilateral fiber optic system consisting of a 500 µm core, 0.63 NA patch cord (Prizmatix) connected to the implanted ferrules. This cord was linked via an FC/PC adaptor and rotary joint (Prizmatix) to a secondary patch cord with a 1500 µm core and 0.63 NA (Prizmatix), which connected to the LED source. Stimulation parameters were set to 5 ms pulses at 20 Hz, with light intensity adjusted to ~3–5 mW at the fiber tip using a digital power meter (ThorLabs).

Chemogenetic stimulation: Mice expressing a DREADD or eYFP control virus received DCZ injections (3 µg/kg, Tocris) or equal volume of saline vehicle intraperitoneally ~30 min prior to the start of a limited-access high-fat

exposure. All mice were habituated with a saline injection in the morning for the 2 days prior to experimental manipulations.

Electrophysiology: Coronal brain slices containing the NAc (250 µm) were prepared from 3 to 4.5-month-old mice, at least 4 weeks following viral injection. Mice were deeply anesthetized with isoflurane and transcardially perfused with ice-cold artificial cerebrospinal fluid (aCSF) containing: 124 mM NaCl, 4 mM KCl, 26 mM $NaHCO_3$, 1 mM Na_2HPO_4, 10 mM glucose, 2 mM $CaCl_2$, and 1.2 mM $MgSO_4$, saturated with 95% O_2 / 5% CO_2. Slices were cut on a microslicer (VT1200S, Leica) in ice-cold high-sucrose cutting solution composed of 254 mM sucrose, 1.25 mM NaH_2PO_4, 24 mM $NaHCO_3$, 3 mM KCl, 2 mM $CaCl_2$, 2 mM $MgCl_2$, and 10 mM glucose, also saturated with 95% O_2 / 5% CO_2. Slices were then transferred to a recovery chamber containing oxygenated aCSF (95% O_2 / 5% CO_2) and allowed to recover for 1 hour at 32 °C. Whole-cell patch-clamp recordings were performed at room temperature (21–22 °C) from $eYFP^+$, $mCherry^+$, or $eGFP^+$ neurons using thin-walled borosilicate glass pipettes (Warner Instruments) with resistance values of 4–7 MΩ. For whole-cell current-clamp recordings, pipettes were filled with an internal solution containing: 115 mM potassium gluconate, 20 mM KCl, 1.5 mM $MgCl_2$, 10 mM phosphocreatine-Tris, 10 mM HEPES, 0.1 mM EGTA, 2 mM Mg-ATP, and 0.5 mM Na-GTP (pH 7.3). To validate hM3Dq and hM4Di expression, deschloroclazapine (DCZ, 250 nM) was bath-applied while neurons were allowed to be at their resting membrane potential (RMP), and changes in RMP were assessed 3 minutes post-application.

Fiber photometry: GCaMP6m signals were collected by a Tucker-Davis Technologies (TDT) fiber photometry system that uses two light-emitting diodes at 460nm (GCaMP6m excitation) and 405nm reflected off dichroic mirrors and coupled into a 400-µm 0.66 N.A. optical fiber (Doric) using Synapse software for signal acquisition. Signal analysis for event detections was performed with custom-written MATLAB software based on previously described methods (Bruno et al., 2021) using an event threshold detection value of 3 standard deviations.

Experimental Design and Statistical Analyses: For all data acquisition and analyses in this study, investigators were blinded to the manipulation that the experimental subject had received and the genotype of the subject. Student's t-tests two-tailed were used when comparing only two groups unless otherwise stated. Two-way ANOVA was used for analysis of multiple groups with Sidak's or Tukey's multiple comparison post-hoc test, when appropriate. Statistical analyses were performed using Prism 10.0 (GraphPad Software). All data were tested and shown to exhibit normality and equal variances. All data are expressed as mean ± s.e.m.

Results

To determine how medial NAc MSN subtype activity regulates high-fat intake during short-term repeated exposure in sated mice, we utilized optogenetics, chemogenetics, and Cre driver lines to modulate D1-MSN or D2-MSN activity. To acutely increase D1-MSN activity, we injected an AAV expressing the conditional activating opsin variant channelrhodopsin H134R (DIO-ChR2) or control virus (DIO-eYFP) into the NAc of D1-Cre mice and performed a limited access exposure to a high-fat diet (**Figure 1A**). Mice were exposed to a high-fat pellet on day 1 with no light stimulation. Mice then received 20 Hz blue light stimulation (5 ms pulse width; 460 nm) bilaterally into the NAc continuously throughout the 20 min high-fat exposure on days 2-4 (**Figure 1A**). Activation of NAc D1-MSNs in ChR2 expressing mice resulted in an overall decrease in total cumulative cal/g of high-fat consumed (**Figure 1B**), and decreased intake in cal/g on day 4 (**Figure 1C**), with no change in body weight (BW) compared to eYFP controls (**Figure 1D**).

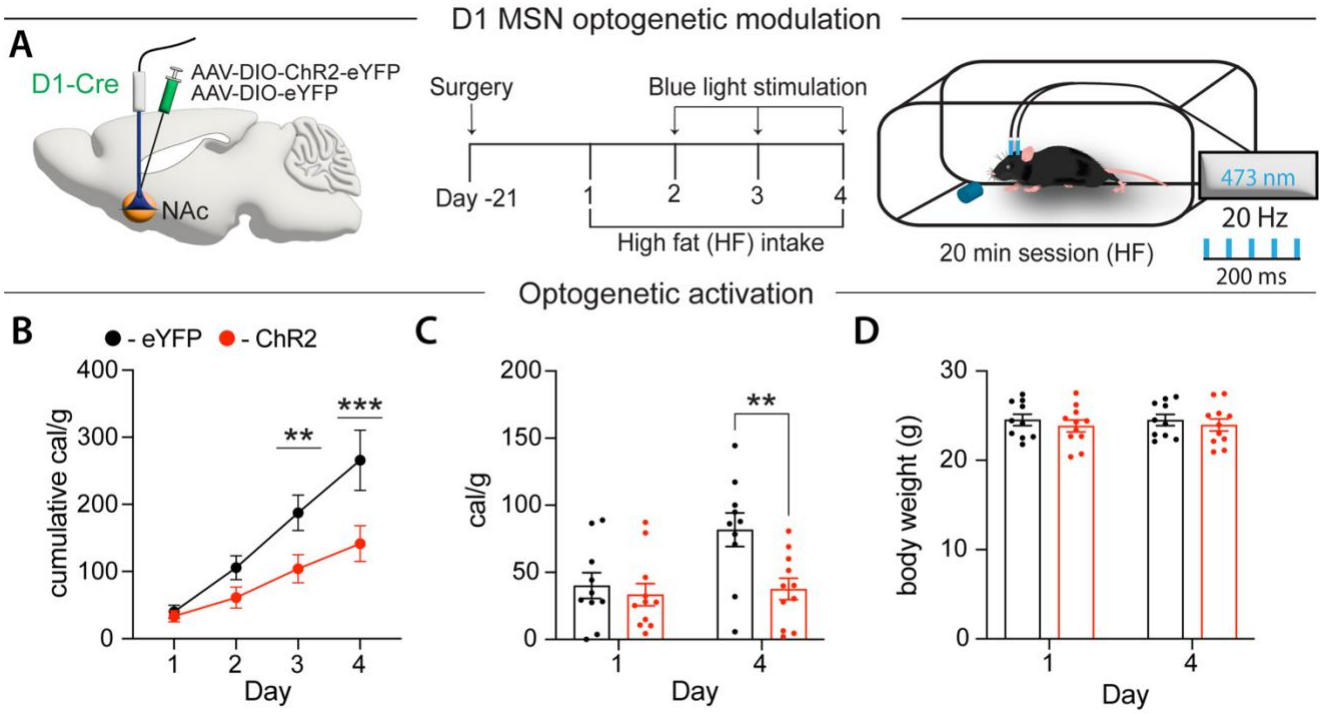

Figure 1. **A**) Schematic of surgery for ChR2 expression (left) and experimental design for D1-MSN experiments (right). Quantification of high-fat intake with optogenetic activation in eYFP control (black) and ChR2 (red) expressing mice as **B**) cumulative intake ($F_{3,57}$ = 5.892, P < 0.001, n = 10, 11 mice/group), and **C**) daily intake in cal/g ($F_{1,19}$ = 5.002, P < 0.05, n = 10, 11 mice/group). **D**) Quantification of body weight on days 1 & 4 ($F_{1,19}$ = 0.316, P = 0.58, n = 10, 11 mice/group). Data are shown as mean ± s.e.m. **P < 0.01, ***P < 0.001, two-way ANOVA with Sidak's multiple comparison post hoc test.

We then confirmed and expanded upon these optogenetic findings using a chemogenetics approach. We injected either the activating DREADD (DIO-hM3Dq-mCitrine) or control virus (DIO-eYFP) into the NAc of D1-Cre mice and again performed a limited access exposure to a high-fat diet. On day 1, mice received a saline injection 30 min prior to high-fat exposure, to assess basal intake in both groups. Mice then received injections of DCZ (3µg/kg) on days 2-4 of exposure (**Figure 2A**). We again found that activation of D1-MSNs decreases total

cumulative cal/g of high-fat consumed and intake on day 4 in hM3Dq expressing mice compared to controls (**Figure 2B, C**) while having no effects on BW (**Figure 2D**)

To decrease D1-MSN activity, we injected the conditional inhibitory DREADD (DIO-hM4Di-mCitrine) or control virus (DIO-eYFP) into the NAc of D1-Cre mice and performed a limited access exposure to a high-fat diet (**Figure 2A**). Here we find that inhibition of D1-MSNs increased overall intake and specifically on day 4 in hM4Di expressing mice compared to controls (**Figure 2E,F**). Once again, no changes in BW were observed in any condition (**Figure 2G**).

To validate our *in vivo* chemogenetics manipulations, we systemically administered DCZ (3μg/kg) to mice expressing hM3Dq, hM4Di, or eYFP. Brains were collected for verification of altered neuronal activity 90 min post administration (**Figure 3A**). Changes in neuronal activity were assessed by cFos expression in virally infected cells (**Figure 3B**). We found an increase in cFos+/eYFP+ cells in hM3Dq-expressing mice compared to controls (**Figure 3C**). Further, we functionally validated our chemogenetic manipulation using whole-cell recordings of hM3Dq expressing MSNs in acute coronal slices. Current clamp recordings confirmed that activation of hM3Dq expressing MSNs resulted in depolarizing the membrane potential and increased spiking (**Figure 3D**). Employing the same experimental design, we verified reduced neuronal activity in our inhibition experiments using hM4Di and found a decrease in cFos+/eYFP+ cells in hM4Di-expressing mice compared to controls and that DCZ application onto hM4Di expressing MSNs decreased membrane potential (**Figure 3E, F**).

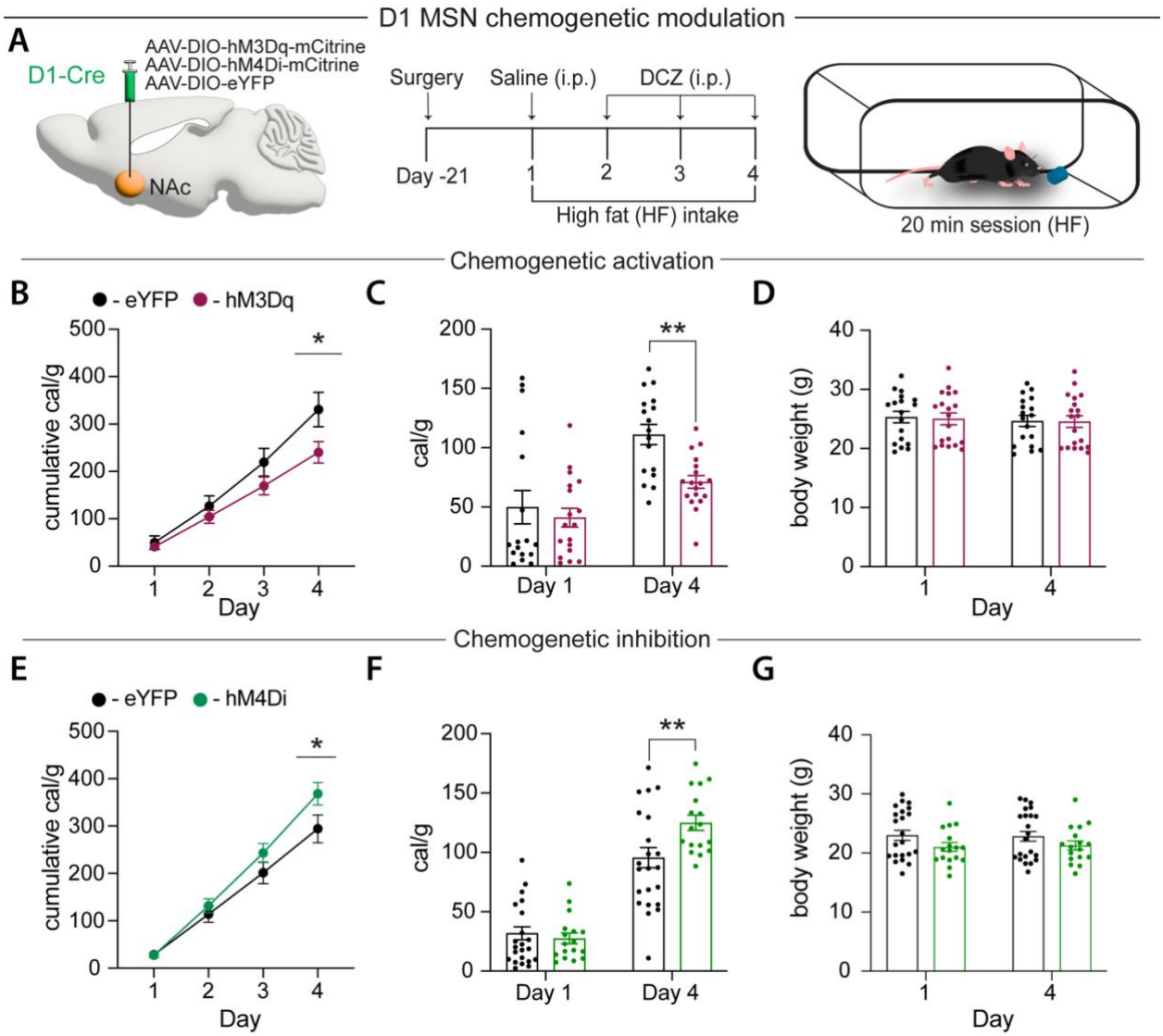

Figure 2. **A**) Schematic of surgery for DREADD expression (left) and experimental design for D1-MSN experiments (right). Quantification of high-fat intake with chemogenetic modulation in eYFP control (black) and hM3Dq (magenta) expressing mice for **B**) cumulative intake ($F_{3,99} = 7.711$, $P < 0.001$, n = 17, 18 mice/group), and **C**) daily intake in cal/g ($F_{1,33} = 7.774$, $P < 0.01$, n = 17, 18 mice/group). **D**) Quantification of body weight on days 1 & 4 ($F_{1,33} = 1.599$, $P = 0.21$, n = 17, 18 mice/group). **E**) Quantification of high-fat intake in eYFP control (black) and hM4Di (green) expressing mice for cumulative intake ($F_{3,111} = 4.633$, $P < 0.01$, n = 22, 17 mice/group), and **F**) daily intake in cal/g ($F_{1,37} = 10.42$, $P < 0.01$, n = 22, 17 mice/group). **G**) Quantification of body weight on days 1 & 4 ($F_{1,37} = 1.542$, $P = 0.22$, n = 22, 17 mice/group). Data are shown as mean ± s.e.m. *P < 0.05, **P < 0.01, two-way ANOVA with Sidak's multiple comparison post hoc test.

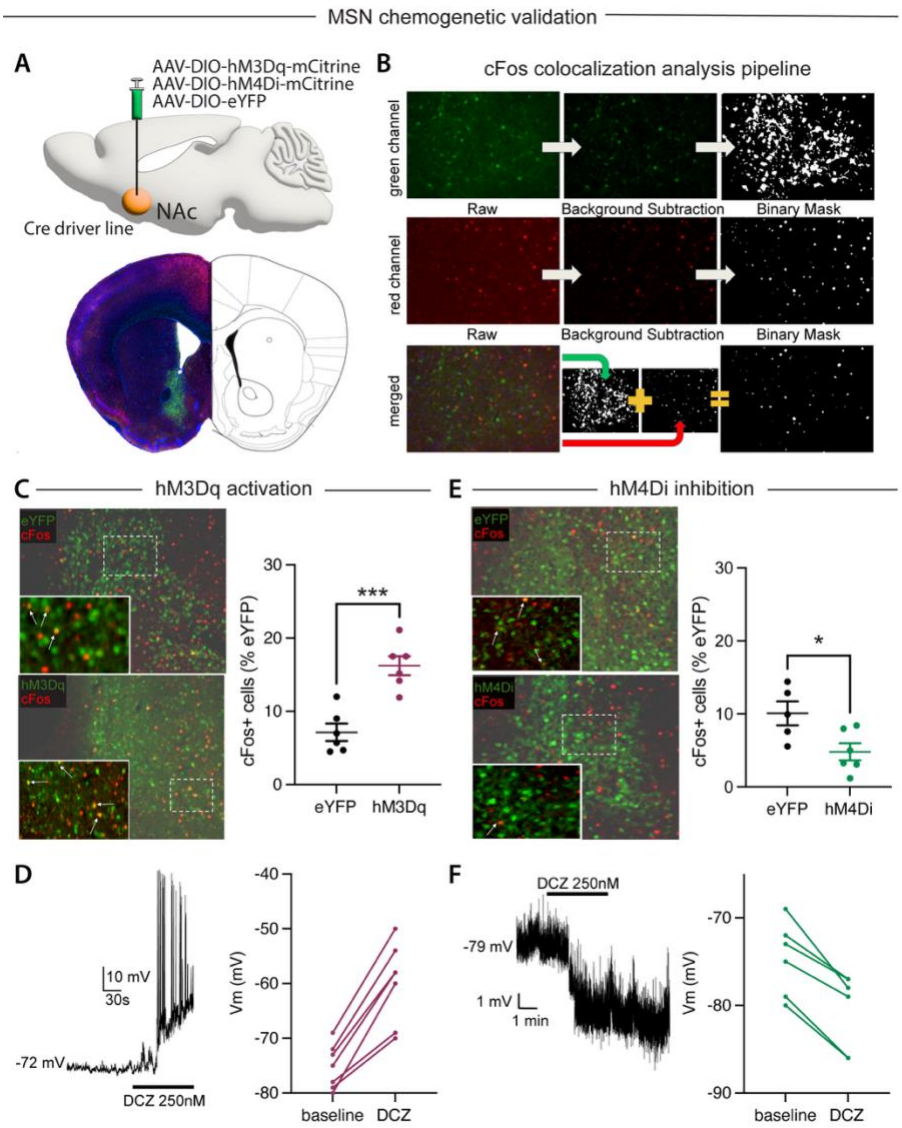

Figure 3. **A**) Schematic of surgery for DREADD expression (top) and representative image of DREADD expression (bottom). **B**) Schematic of analysis pipeline for quantification of cFos+ virally infected MSNs. **C**) Representative images of eYFP and hM3Dq expression (green) co-stained for cFos (red). White arrows indicate cFos+ neurons colocalized with virus (left). Quantification of the percent of eYFP+ cells that are cFos+ in eYFP control (black) and hM3Dq (magenta) expressing mice (right; $t_{(10)}$ = 5.16, p = 0.0004, n = 6 mice/group). **D**) Representative trace of current clamp recordings in hM3Dq+ MSNs (left). Quantification of membrane voltage at baseline and following bath application of DCZ (right; $t_{(6)}$ = 4.505, p = 0.0004, n = 7 mice/group). **E**) Representative images of eYFP and hM4Di expression co-stained for cFos (red). White arrows indicate cFos+ neurons colocalized with virus (left). Quantification of the percent of eYFP+ cells that are cFos+ in eYFP control (black) and hM4Di (green) expressing mice (right; $t_{(9)}$ =2.678, p = 0.025, n = 6,5 mice/group) **F**) Representative trace of current clamp recordings in hM4Di+ MSNs (left). Quantification of membrane voltage at baseline and following bath application of DCZ (right; $t_{(5)}$ = 3.15 p = 0.0255, n = 6 mice/group). Data are shown as mean ± s.e.m. *P < 0.05, ***P < 0.001, student's paired t-test.

We next probed the effects of manipulating D2-MSN activating by injecting an AAV-DIO-hM3Dq-mCitrine or AAV-DIO-eYFP control into the NAc of A2a-Cre mice and performed our limited access high-fat exposure paradigm (**Figure 4A**). Activation of medial NAc D2-MSNs resulted in a significant overall increase in cumulative cal/g (**Figure 4B**) and intake on day 4 (**Figure 4C**) with no change in BW in hM3Dq expressing mice compared to controls (**Figure 4D**).

To complete our investigations of bidirectional modulation of MSN subtype activity, we injected AAV-DIO-hM4Di-mCitrine or AAV-DIO-eYFP control virus into the NAc of A2a-Cre mice and assayed the effect of D2-MSN inhibition on high-fat intake (**Figure 4A**). Inhibition of D2-MSNs resulted in a robust decrease in overall

intake (**Figure 4E**) and daily consumption on day 4 (**Figure 4F**), to a larger degree than D1-MSN activation, without perturbing BW (**Figure 4G**).

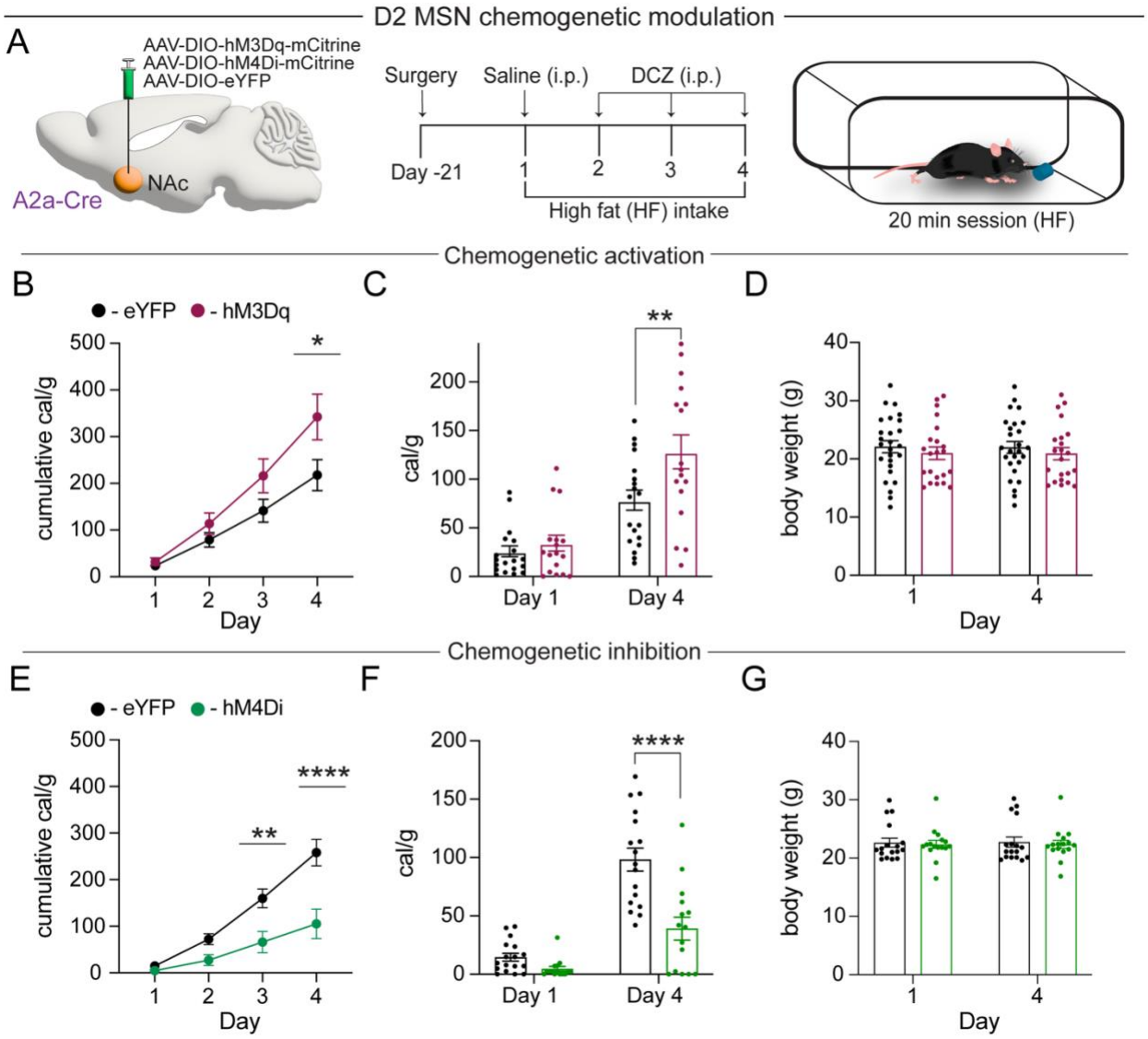

Figure 4. **A**) Schematic of surgery for DREADD expression (left) and experimental design for D2-MSN experiments (right). Quantification of high-fat intake with chemogenetic modulation in eYFP control (black) and hM3Dq (magenta) expressing mice for **B**) cumulative intake ($F_{3,102} = 5.014$, $P < 0.01$, n = 19, 17 mice/group), and **C**) daily intake in cal/g ($F_{1,34} = 5.428$, $P < 0.05$, n = 19,17 mice/group). **D**) Quantification of body weight on days 1 & 4 ($F_{1,34} = 0.113$, $P = 0.73$, n = 19,17 mice/group). **E**) Quantification of high-fat intake in eYFP control (black) and hM4Di (green) expressing mice for cumulative intake ($F_{3,90} = 12.27$, $P < 0.0001$, n = 17, 15 mice/group), and **F**) daily intake in cal/g (mice ($F_{1,30} = 16.02$, $P < 0.0001$, n = 17,15 mice/group), **G**) Quantification of body weight on days 1 & 4 (mice ($F_{1,30} = 0.11347$, $P = 0.71$, n = 17,15 mice/group). Data are shown as mean ± s.e.m. *P < 0.05, **P < 0.01, ****P < 0.0001, two-way ANOVA with Sidak's multiple comparison post hoc test.

Previous reports find that D2-MSN activity is not significantly altered during bouts of binge eating following ten days of high-fat exposure (Wu et al., 2022), yet population activity of D2-MSNs is increased during consumption of palatable sweet milk (Walle et al., 2024) . Given the robust effects of chemogenetic modulation of NAc D2-MSNs on high-fat intake we observed, we performed photometric recordings of NAc D2-MSNs during the 1st and 4th day of high-fat exposure. We injected AAV-DIO-GCaMP6m into the NAc of A2a-Cre mice and recorded

population activity of D2-MSNs Ca^{2+} transients during both a baseline condition where no high-fat pellet was present and during high-fat exposure (**Figure 5A, B**). We found that following 4 days of exposure there are no changes in the frequency of Ca^{2+} transients at baseline but an increase in the frequency of events during exposure to high-fat (**Figure 5C**). Further, when we normalized Ca^{2+} transient frequency during high-fat exposure to baseline rates we found a robust change in the pattern of D2-MSN activity. While D2-MSN activity decreases during high-fat exposure on day 1 compared to baseline, it robustly increases during exposure on day 4, when intake is also significantly increased (**Figure 5D, E**).

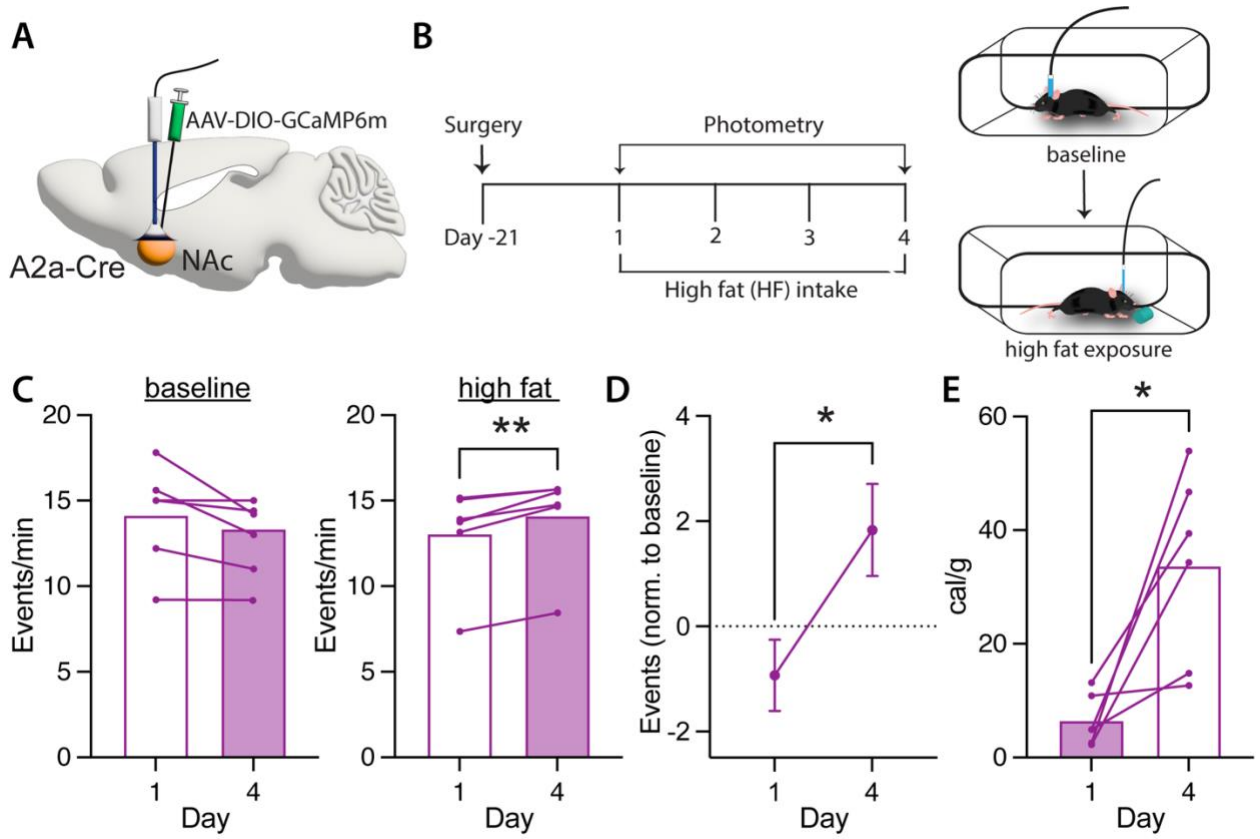

Figure 5. **A**) Schematic of surgery for GCaMP6m expression and fiber optic implantation in A2a-Cre mice. **B**) Experimental design for D2-MSN fiber photometry experiments. **C**) Quantification of D2-MSN Ca^{2+} transient frequency during baseline (left: $t_{(5)} = 2.326$, $p = 0.0675$, n = 6 mice) and high-fat exposure (right: $t_{(5)} = 5.165$, $p < 0.01$, n = 6 mice) and **D**) normalized event frequency on days 1 and 4 ($t_{(5)} = 4.238$, $p < 0.01$, n = 6 mice). **E**) Quantification of high-fat intake on days 1 and 4 ($t_{(5)} = 3.545$, $p < 0.01$, n = 6 mice). Data are shown as mean ± s.e.m. *P < 0.05, **P < 0.01, student's paired t-test.

Discussion

These findings support a critical role for MSNs in the NAc in the regulation of hedonic feeding and reveal opposing contributions of D1- and D2-MSNs to high-fat food intake. Selective activation of D1-MSNs significantly reduced consumption of high-fat food, suggesting that these neurons may contribute to the suppression of hedonic feeding, potentially by signaling satiety or mediating negative feedback associated with overconsumption. In contrast, activation of D2-MSNs increased high-fat food intake, indicating a facilitatory or disinhibitory role in the consumption of palatable food. These results are consistent with prior reports demonstrating that inhibition of NAc neurons promotes feeding, whereas brief activation can disrupt ongoing

consumption. Together, these findings extend current models of NAc function by implicating its medial subregion as a critical integrative hub for the coordination of homeostatic and reward-driven feeding behavior.

The observed suppression of high-fat food intake by D1-MSN activation aligns with recent research that elucidates the distinct contributions of D1- and D2-MSNs to reward processing and their dissociable roles in motivated behavior (Richard et al., 2013; Marinescu and Labouesse, 2024). Many studies support a direct link between D1-MSN activity and feeding likely through their output pathways to the lateral hypothalamus (LH), ventral tegmental area (VTA), and ventral pallidum (Castro and Bruchas, 2019; Ferrario et al., 2024). Optogenetic inhibition of D1-MSNs permits feeding, while activation of their terminals in the LH rapidly suppresses ongoing consumption, even in food restricted mice (O'Connor et al., 2015). Similarly, we find that optogenetic activation of NAc D1-MSNs decreases cumulative high-fat food intake, and others demonstrate that the medial NAc→VTA projection bidirectionally regulates feeding, with D1-MSNs being the primary neuronal subtype projecting to the VTA (Bond et al., 2020) .

Yet, the effect on D1-MSN activity on eating appears to depend on the diet (high-calorie palatable vs standard chow), length of exposure to calorically dense diets, and whether MSN subtype activity is manipulated acutely or chronically. Recent work by Matikainen-Ankney et al. demonstrates that high-fat diet-induced obesity preferentially enhances excitatory synaptic input onto NAc core D1-MSNs, but not D2-MSNs. This enhancement is characterized by an increase in the frequency of miniature excitatory postsynaptic currents and elevated intrinsic excitability of D1-MSNs (Matikainen-Ankney et al., 2023). However, acute activation of D1-MSNs in the NAc core enhances motivation for a food reward while paradoxically decreasing high-fat intake, while the opposite manipulation increases it (Walle et al., 2024). Recent sequencing and transcriptomic studies have shown significant heterogeneity within the MSN subtypes classified by their dopamine receptor, adding another layer of complexity to understanding their role in feeding (Gokce et al., 2016; Chen et al., 2021; He et al., 2021). A specific subpopulation of NAc D1-MSNs, marked by expression of SERPINB2, was found to bidirectionally control food intake and energy balance by projecting to leptin receptor-expressing neurons in the LH. Activation of these neurons increases food intake without influencing other behaviors, suggesting they could be targeted for treating obesity or eating disorders (Liu et al., 2024). Altogether, this evidence reinforces the idea that D1-MSNs are crucial for regulating food intake and yet highlights the need to comprenhend the nuanced contributions of their activity to in various aspects of feeding and eating disorders.

There is less evidence that D2-MSNs directly modulate intake in a reliable manner (O'Connor et al., 2015; Zhu et al., 2016; Matikainen-Ankney et al., 2023; Walle et al., 2024; Requejo-Mendoza et al., 2025). However, clinical and preclinical studies find that alterations in D2 receptor levels and function are linked to altered intake and body weight (Johnson and Kenny, 2010; Kenny, 2011; Volkow et al., 2011, 2017; DiFeliceantonio and Small, 2019).

Further, increasing or decreasing D2 receptor expression or activity in D2-MSNs leads to decreased or increased excitability of these neurons (Perez et al., 2006; Cazorla et al., 2012; Planert et al., 2013). During feeding, D2-MSNs have been found to be more active, and chemogenetic activation or inhibition can increase or decrease food intake, in agreement with our findings (Zhu et al., 2016; Walle et al., 2024). Further, upregulation of striatal D2 receptorss regulates susceptibility to diet-induced obesity (Labouesse et al., 2018). These types of alterations in D2-MSN activity are thought to influence weight-gain and the development of obesity primarily via modulation of energy expenditure. Ultimately, the balance between D1- and D2-MSN activity in the NAc may differentially regulate the decision to engage in feeding versus voluntary exercise, providing a potential mechanistic link to the "metabo-psychiatric" nature of eating disorders (Hardaway et al., 2015; Initiative et al., 2019; Bulik et al., 2021; Hickey and Matikainen-Ankney, 2025).

The activity of NAc MSNs is primarily driven glutamatergic inputs from regions, including the amygdala, hippocampus, thalamic, and cortical structures (MacAskill et al., 2012; Klawonn and Malenka, 2018; Christoffel et al., 2021b). The ventral hippocampus (vHipp), basolateral amygdala (BLA), paraventricular nucleus of the thalamus (PVT), and medial prefrontal cortex (mPFC) are all identified as feeding-related excitatory inputs to the NAc shell (Kelley et al., 2005; Sweeney and Yang, 2015; Ong et al., 2017; Castro and Bruchas, 2019; Christoffel et al., 2021a). Optogenetic inhibition of vHipp inputs to the NAc shell strongly promotes feeding, suggesting these inputs normally inhibit food consumption by dampening NAc shell activity (Reed et al., 2018). Similarly, inhibition of mPFC→NAc neurons has been shown to significantly increase high-fat intake. Conversely, inhibition of anterior PVT (aPVT) inputs to the NAc decreases high-fat intake. The medial NAc also receives direct inputs from the LH, including orexin and melanin-concentrating hormone (MCH) populations, providing unique access to metabolic and motivational information. Further, visceral information is relayed by the caudal nucleus of the solitary tract (NTS) which could regulate motivated and stress-related behaviors (Castro and Bruchas, 2019). This highlights the complexity of the diverse signals integrated by MSNs that lead to their regulation of feeding.

The NAc's role extends beyond merely modulating food intake to influencing different aspects of reward. While NAc core mu-opioid receptors (MORs) primarily promote food seeking rather than consumption itself (Caref and Nicola, 2018), the NAc shell projection neurons are thought to primarily control the onset and offset of food consumption, independent of metabolic need (Marinescu and Labouesse, 2024). Electrophysiological recordings in the NAc show that certain neurons exhibit short-lived excitation during food consumption, especially with palatable rewards, reflecting sensory and value encoding. Other neurons exhibit prolonged inhibition during consumption, tracking the motor act of licking rather than the food's sensory properties (Taha and Fields, 2005, 2006; Krause et al., 2010). This suggests that MSN activity, when modulated as shown in our findings, is influencing these consumption-related neural signals. The activity of endogenous opioids, which are proposed to

be enhanced by insulin receptor activation on MSNs, can also disinhibit presynaptic glutamate release in the NAc, further complicating the network's regulation of feeding (Fetterly et al., 2021).

The opposing effects of D1- and D2-MSN activation on high-fat food intake underscore the NAc as a key regulator of motivated feeding behavior, modulating the hedonic value of food independent of homeostatic need. These findings align with prior evidence demonstrating that projections from the NAc shell can drive both hyperphagia and hypophagia regardless of hunger state. Future studies should aim to further delineate the functional specificity of D1- and D2-MSNs within NAc subregions, taking into account the molecular heterogeneity of these neurons, the diversity of afferent inputs, and the influence of neuromodulatory systems. Elucidating how these complex circuits govern the consumption of palatable food will be critical for understanding the neural mechanisms underlying maladaptive eating and may provide novel targets for therapeutic intervention in obesity and related metabolic disorders.

References:

Bond CW, Trinko R, Foscue E, Furman K, Groman SM, Taylor JR, DiLeone RJ (2020) Medial Nucleus Accumbens Projections to the Ventral Tegmental Area Control Food Consumption. J Neurosci 40:4727–4738.

Brown R, Kupchik Y, Spencer S, Garcia-Keller C, Spanswick DC, Lawrence A, Simonds S, Schwartz D, Jordan K, Jhou T, Kalivas P (2015) Addiction-like synaptic impairments in diet-induced obesity. Bio Psych 9:797–806.

Bruno CA, O'Brien C, Bryant S, Mejaes JI, Estrin DJ, Pizzano C, Barker DJ (2021) pMAT: An open-source software suite for the analysis of fiber photometry data. Pharmacol Biochem Be 201:173093.

Bulik CM, Carroll IM, Mehler P (2021) Reframing anorexia nervosa as a metabo-psychiatric disorder. Trends Endocrinol Metab 32:752–761.

Caref K, Nicola SM (2018) Endogenous opioids in the nucleus accumbens promote approach to high-fat food in the absence of caloric need. eLife 7:e34955.

Castro DC, Bruchas MR (2019) A Motivational and Neuropeptidergic Hub: Anatomical and Functional Diversity within the Nucleus Accumbens Shell. Neuron 102:529–552.

Cazorla M, Shegda M, Ramesh B, Harrison NL, Kellendonk C (2012) Striatal D2 Receptors Regulate Dendritic Morphology of Medium Spiny Neurons via Kir2 Channels. J Neurosci 32:2398–2409.

Chen R, Blosser TR, Djekidel MN, Hao J, Bhattacherjee A, Chen W, Tuesta LM, Zhuang X, Zhang Y (2021) Decoding molecular and cellular heterogeneity of mouse nucleus accumbens. Nat Neurosci 24:1757–1771.

Christoffel DJ, Walsh JJ, Heifets BD, Hoerbelt P, Neuner S, Sun G, Ravikumar VK, Wu H, Halpern CH, Malenka RC (2021a) Input-specific modulation of murine nucleus accumbens differentially regulates hedonic feeding. Nat Commun 12:2135.

Christoffel DJ, Walsh JJ, Hoerbelt P, Heifets BD, Llorach P, Lopez RC, Ramakrishnan C, Deisseroth K, Malenka RC (2021b) Selective filtering of excitatory inputs to nucleus accumbens by dopamine and serotonin. Proc National Acad Sci 118:e2106648118.

DiFeliceantonio AG, Small DM (2019) Dopamine and diet-induced obesity. Nat Neurosci 22:1–6.

Ferrario CR (2017) Food Addiction and Obesity. Neuropsychopharmacology 42:361–361.

Ferrario CR, Münzberg-Gruening H, Rinaman L, Betley JN, Borgland SL, Dus M, Fadool DA, Medler KF, Morton GJ, Sandoval DA, Serre CB de L, Stanley SA, Townsend KL, Watts AG, Maruvada P, Cummings D, Cooke BM (2024) Obesity- and diet-induced plasticity in systems that control eating and energy balance. Obesity 32:1425–1440.

Fetterly TL, Oginsky MF, Nieto AM, Alonso-Caraballo Y, Santana-Rodriguez Z, Ferrario CR (2021) Insulin Bidirectionally Alters NAc Glutamatergic Transmission: Interactions between Insulin Receptor Activation, Endogenous Opioids, and Glutamate Release. J Neurosci 41:2360–2372.

Gokce O, Stanley GM, Treutlein B, Neff NF, Camp JG, Malenka RC, Rothwell PE, Fuccillo MV, Südhof TC, Quake SR (2016) Cellular Taxonomy of the Mouse Striatum as Revealed by Single-Cell RNA-Seq. Cell Rep 16:1126–1137.

Hardaway J, Crowley N, Bulik C, Kash T (2015) Integrated circuits and molecular components for stress and feeding: implications for eating disorders. Genes, Brain and Behavior 14:85–97.

He J, Kleyman M, Chen J, Alikaya A, Rothenhoefer KM, Ozturk BE, Wirthlin M, Bostan AC, Fish K, Byrne LC, Pfenning AR, Stauffer WR (2021) Transcriptional and anatomical diversity of medium spiny neurons in the primate striatum. Curr Biol 31:5473-5486.e6.

Hickey AKS, Matikainen-Ankney BA (2025) Endogenous opioid receptors and the feast or famine of maladaptive feeding. Nat Commun 16:2270.

Initiative A et al. (2019) Genome-wide association study identifies eight risk loci and implicates metabo-psychiatric origins for anorexia nervosa. Nature Genetics 51:1207–1214.

Johnson PM, Kenny PJ (2010) Dopamine D2 receptors in addiction-like reward dysfunction and compulsive eating in obese rats. Nat Neurosci 13:635–641.

Kelley AE (2004) Ventral striatal control of appetitive motivation: role in ingestive behavior and reward-related learning. Neuroscience and biobehavioral reviews 27:765–776.

Kelley AE, Baldo BA, Pratt WE (2005) A proposed hypothalamic-thalamic-striatal axis for the integration of energy balance, arousal, and food reward. J Comp Neuro 493:72–85.

Kenny PJ (2011) Common cellular and molecular mechanisms in obesity and drug addiction. Nat Rev Neuro 12:638–651.

Klawonn AM, Malenka RC (2018) Nucleus Accumbens Modulation in Reward and Aversion. Cold Spring Harb Sym 83:119–129.

Krause M, German PW, Taha SA, Fields HL (2010) A pause in nucleus accumbens neuron firing is required to initiate and maintain feeding. J Neurosci 30:4746–4756.

Labouesse MA, Sartori AM, Weinmann O, Simpson EH, Kellendonk C, Weber-Stadlbauer U (2018) Striatal dopamine 2 receptor upregulation during development predisposes to diet-induced obesity by reducing energy output in mice. Proceedings of the National Academy of Sciences:201800171.

Liu Y, Wang Y, Zhao Z, Xie G, Zhang C, Chen R, Zhang Y (2024) A subset of dopamine receptor-expressing neurons in the nucleus accumbens controls feeding and energy homeostasis. Nat Metab 6:1616–1631.

MacAskill AF, Little JP, Cassel JM, Carter AG (2012) Subcellular connectivity underlies pathway-specific signaling in the nucleus accumbens. Nat Neurosci 15:1624–1626.

Marinescu A-M, Labouesse MA (2024) The nucleus accumbens shell: a neural hub at the interface of homeostatic and hedonic feeding. Front Neurosci 18:1437210.

Matikainen-Ankney BA, Legaria AA, Pan Y, Vachez YM, Murphy CA, Schaefer RF, McGrath QJ, Wang JG, Bluitt MN, Ankney KC, Norris AJ, Creed MC, Kravitz AV (2023) Nucleus Accumbens D1 Receptor–Expressing Spiny Projection Neurons Control Food Motivation and Obesity. Biol Psychiatry 93:512–523.

Mogenson GJ, Jones DL, Yim C (1980) From motivation to action: Functional interface between the limbic system and the motor system. Prog Neurobiol 14:69–97.

O'Connor EC, Kremer Y, Lefort S, Harada M, Pascoli V, Rohner C, Lüscher C (2015) Accumbal D1R neurons projecting to lateral hypothalamus authorize feeding. Neuron 88:553–564.

Oginsky MF, Ferrario CR (2019) Eating "junk food" has opposite effects on intrinsic excitability of nucleus accumbens core neurons in obesity-susceptible versus -resistant rats. J Neurophysiol 122:1264–1273.

Ong ZY, Liu J-J, Pang ZP, Grill HJ (2017) Paraventricular thalamic control of food intake and reward: Role of glucagon-like peptide-1 receptor signaling. Neuropsychopharm 42:2387–2397.

Perez MF, White FJ, Hu X-TT (2006) Dopamine D(2) receptor modulation of K(+) channel activity regulates excitability of nucleus accumbens neurons at different membrane potentials. Journal of neurophysiology 96:2217–2228.

Planert H, Berger TK, Silberberg G (2013) Membrane Properties of Striatal Direct and Indirect Pathway Neurons in Mouse and Rat Slices and Their Modulation by Dopamine. PLoS ONE 8:e57054.

Reed SJ, Lafferty CK, Mendoza JA, Yang AK, Davidson TJ, Grosenick L, Deisseroth K, Britt JP (2018) Coordinated reductions in excitatory input to the nucleus accumbens underlie food consumption. Neuron 6:1260–1273.

Requejo-Mendoza N, Arias-Montaño J-A, Gutierrez R (2025) Nucleus accumbens D2-expressing neurons: Balancing reward and licking disruption through rhythmic optogenetic stimulation. PLOS ONE 20:e0317605.

Richard J, Castro D, DiFeliceantonio A (2013) Mapping brain circuits of reward and motivation: in the footsteps of Ann Kelley.

Roitman MF, Wheeler RA, Carelli RM (2005) Nucleus Accumbens Neurons Are Innately Tuned for Rewarding and Aversive Taste Stimuli, Encode Their Predictors, and Are Linked to Motor Output. Neuron 45:587–597.

Russo SJ, Nestler EJ (2013) The brain reward circuitry in mood disorders. Nature Reviews Neuroscience 14:609–625.

Sharma S, Fernandes M, Fulton S (2012) Adaptations in brain reward circuitry underlie palatable food cravings and anxiety induced by high-fat diet withdrawal. Int J Obesity 37:1183–1191.

Steinberg EE, Christoffel DJ, Deisseroth K, Malenka RC (2015) Illuminating circuitry relevant to psychiatric disorders with optogenetics. Current opinion in neurobiology 30:9–16.

Sweeney P, Yang Y (2015) An excitatory ventral hippocampus to lateral septum circuit that suppresses feeding. Nature Communications 6.

Taha S, Fields H (2005) Encoding of palatability and appetitive behaviors by distinct neuronal populations in the nucleus accumbens. J Neurosci:1193–1202.

Taha SA, Fields HL (2006) Inhibitions of Nucleus Accumbens Neurons Encode a Gating Signal for Reward-Directed Behavior. J Neurosci 26:217–222.

Valdivia S, Patrone A, Reynaldo M, Perello M (2014) Acute High Fat Diet Consumption Activates the Mesolimbic Circuit and Requires Orexin Signaling in a Mouse Model. PLoS ONE 9:e87478.

Volkow ND, Wang G-J, Baler RD (2011) Reward, dopamine and the control of food intake: implications for obesity. Trends in Cognitive Sciences 15:37–46.

Volkow ND, Wise RA (2005) How can drug addiction help us understand obesity? Nat Neurosci 8:555–560.

Volkow ND, Wise RA, Baler R (2017) The dopamine motive system: implications for drug and food addiction. Nat Rev Neuro 18:741–752.

Walle R et al. (2024) Nucleus accumbens D1- and D2-expressing neurons control the balance between feeding and activity-mediated energy expenditure. Nat Commun 15:2543.

Wu H, Kakusa B, Neuner S, Christoffel DJ, Heifets BD, Malenka RC, Halpern CH (2022) Local accumbens in vivo imaging during deep brain stimulation reveals a strategy-dependent amelioration of hedonic feeding. Proc National Acad Sci 119:e2109269118.

Wu H, Miller KJ, Blumenfeld Z, Williams NR, Ravikumar VK, Lee KE, Kakusa B, Sacchet MD, Wintermark M, Christoffel DJ, Rutt BK, Bronte-Stewart H, Knutson B, Malenka RC, Halpern CH (2018) Closing the loop on impulsivity via nucleus accumbens delta-band activity in mice and man. Proc Natl Acad Sci 115:192–197.

Zhu X, Ottenheimer D, DiLeone RJ (2016) Activity of D1/2 receptor expressing neurons in the nucleus accumbens regulates running, locomotion, and food intake. Front Beh Neuro 10:1–10.